

Article

Triphenyltin(IV) Carboxylates with Exceptionally High Cytotoxicity against Different Breast Cancer Cell Lines

Ivana Predarska ^{1,2}, Mohamad Saoud ³, Ibrahim Morgan ³, Peter Lönnecke ¹, Goran N. Kaluđerović ^{2,3,*}
and Evamarie Hey-Hawkins ^{1,*}

¹ Institute of Inorganic Chemistry, Faculty of Chemistry and Mineralogy, Leipzig University, Johannisallee 29, 04103 Leipzig, Germany

² Department of Engineering and Natural Sciences, University of Applied Sciences Merseburg, Eberhard Leibnitz-Str. 2, 06217 Merseburg, Germany

³ Department of Bioorganic Chemistry, Leibniz Institute of Plant Biochemistry, Weinberg 3, 06120 Halle (Saale), Germany

* Correspondence: goran.kaluderovic@hs-merseburg.de (G.N.K.); hey@uni-leipzig.de (E.H.-H.); Tel.: +49-3461-46-2012 (G.N.K.); +49-341-97-36151 (E.H.-H.)

Abstract: Organotin(IV) carboxylates are a class of compounds explored as alternatives to platinum-containing chemotherapeutics due to propitious in vitro and in vivo results, and distinct mechanisms of action. In this study, triphenyltin(IV) derivatives of non-steroidal anti-inflammatory drugs (indomethacin (HIND) and flurbiprofen (HFBP)) are synthesized and characterized, namely [Ph₃Sn(IND)] and [Ph₃Sn(FBP)]. The crystal structure of [Ph₃Sn(IND)] reveals penta-coordination of the central tin atom with almost perfect trigonal bipyramidal geometry with phenyl groups in the equatorial positions and two axially located oxygen atoms belonging to two distinct carboxylato (IND) ligands leading to formation of a coordination polymer with bridging carboxylato ligands. Employing MTT and CV probes, the antiproliferative effects of both organotin(IV) complexes, indomethacin, and flurbiprofen were evaluated on different breast carcinoma cells (BT-474, MDA-MB-468, MCF-7 and HCC1937). [Ph₃Sn(IND)] and [Ph₃Sn(FBP)], unlike the inactive ligand precursors, were found extremely active towards all examined cell lines, demonstrating IC₅₀ concentrations in the range of 0.076–0.200 μM. Flow cytometry was employed to examine the mode of action showing that neither apoptotic nor autophagic mechanisms were triggered within the first 48 h of treatment. However, both tin(IV) complexes inhibited cell proliferation potentially related to the dramatic reduction in NO production, resulting from downregulation of nitric oxide synthase (iNOS) enzyme expression.

Keywords: triphenyltin(IV); indomethacin; flurbiprofen; anticancer; breast cancer; NO production



Citation: Predarska, I.; Saoud, M.; Morgan, I.; Lönnecke, P.; Kaluđerović, G.N.; Hey-Hawkins, E. Triphenyltin(IV) Carboxylates with Exceptionally High Cytotoxicity against Different Breast Cancer Cell Lines. *Biomolecules* **2023**, *13*, 595. <https://doi.org/10.3390/biom13040595>

Academic Editor: Andrey A. Zamyatnin, Jr.

Received: 3 March 2023

Revised: 21 March 2023

Accepted: 22 March 2023

Published: 26 March 2023



Copyright: © 2023 by the authors. Licensee MDPI, Basel, Switzerland. This article is an open access article distributed under the terms and conditions of the Creative Commons Attribution (CC BY) license (<https://creativecommons.org/licenses/by/4.0/>).

1. Introduction

Given that carcinoma is a main cause of death and a significant obstacle to raising life expectancy globally [1–3], it is not a surprise that the prime objective of contemporary medicinal chemistry is the creation of novel anticancer medications. After the unintentional finding of cisplatin in the 1960s [4] and the success it had treating several solid tumors types [5,6], numerous platinum-based compounds have undergone substantial research as potential chemotherapeutics [7–9]. However, the drawbacks related to using platinum-based therapies in clinical settings, such as systemic toxicity as well as innate and/or acquired resistance [10,11], have motivated scientists to expand the investigation also on other possible metal-based chemotherapeutic alternatives potentially exhibiting distinct modes of action. Many different metals, such as Ti, Fe, Ru, Os, Co, Rh, Ir, Pd, Cu, Au, Ga, Ge, and Sn, have spurred considerable attention in this context [12–16]. Among them, organotin(IV) complexes have appeared as very noteworthy non-platinum metallodrugs investigated by many research groups in the past four decades [17–20]. This is due to their reduced toxicity [17] and capacity to circumvent the medication resistance perceived for some commercially available metal-based pharmaceuticals [21].

The potential to induce apoptosis as well as to strongly interact with the deoxyribonucleic acid (DNA) are key for the chemotherapeutic capacity of organotin(IV) complexes [22]. The organic ligand is crucial for the bioactivity of these complexes; thus, Bu and Ph ligands result in more active compounds compared to those bearing Et and Me ligands [13,23]. The relative lipophilicity of the organotin moieties could be responsible for this effect [24]. The ligands' nature is also closely related with the biological activity. Among the extensively studied thiolato [25–30], dithiocarbamate [31], and carboxylate [32–39] ligands, the last ones showed highest cytotoxic activity in vitro [24] and significant reduction in tumor growth in vivo [40,41].

Since it was discovered that the cyclooxygenase (COX) enzyme, particularly the isozyme COX-2, contributes to tumor generation and angiogenesis [42] and is overexpressed in certain tumor cells, such as stomach, colorectal, pancreas, bladder, breast, skin and esophagus [43], both non-steroidal anti-inflammatory drugs (NSAIDs), which are non-selective COX inhibitors, as well as COX-2-selective inhibitors (COXIBs) have been exploited as adjuvant chemotherapeutic and/or chemopreventive agents [44,45]. Complexes of different metals with NSAIDs have been previously prepared and discovered to have significant in vitro anticancer activity [46–53]. Complexes of organotin(IV) with NSAIDs have also been investigated. Triphenyltin(IV) complexes of flufenamic and mefenamic acid, namely triphenyltin(IV) flufenamate and mefenamate, have shown high in vitro cytotoxicity towards A549 (lung carcinoma), T-24 (bladder carcinoma) and MCF-7 (breast carcinoma) cells [54]. Different organotin(IV) ibuprofenate compounds have been synthesized as well and screened in vitro for cytotoxicity against Caco-2 (colorectal adenocarcinoma), HCT-15 (colon adenocarcinoma) and DU145 (prostate carcinoma) cells. According to the findings, triphenyltin(IV) ibuprofenate is most active against the cell line Caco-2 [55]. Oxaprozin is another NSAID used as carboxylate ligand in different di- and triorganotin(IV) complexes whose antiproliferative effects have been examined in vitro on a plethora of carcinoma cells including human colorectal adenocarcinoma (HT-29), hepatocellular (HepG2), breast (MCF-7), and prostate (PC-3) cancer cells. These complexes have shown excellent cytotoxicity with IC_{50} values of 0.10–0.76 μ M. Once again, triphenyltin(IV) oxaprozinate has demonstrated greatest cytotoxicity towards the cancer cell line MCF-7 [56]. Several organotin(IV) indomethacinates have also been prepared; tri-*n*-butyltin(IV) and triphenyltin(IV) indomethacinate exhibited cytotoxic activity against the SK-LU-1 lung adenocarcinoma and the cervical cancer HeLa cells [57]. Additionally, different organotin(IV) derivatives with racemic flurbiprofenate as ligand have been prepared. However, they have only been tested as antibacterial and antifungal agents, while their cytotoxic activity has not been evaluated [58].

Based on the latest cancer statistics, globally the most commonly diagnosed cancer and the number one reason for cancer-related death in women is female breast cancer [2]. Certain forms of breast cancer respond quite well to treatment. Yet, forms such as the triple-negative breast cancer (TNBC, estrogen-, progesterone- and HER-2-negative (ER-, PR-, HER2-)), are exceedingly difficult to medicate because of the disease's complexity and absence of distinct molecular targets [59]. We have previously reported platinum(IV) complexes with different NSAIDs that proved to be highly effective towards different breast cancer cells. The cisplatin-indomethacinate (IND) conjugate was even able to overcome resistance expressed towards cisplatin by MDA-MB-231 breast carcinoma cells [60]. The racemic cisplatin-flurbiprofenate (FBP) conjugate showed even higher cytotoxic potency against four different breast cancer cell lines (MCF-7, HCC-1937, MDA-MB-468, BT-474) [61]. In order to assess how the metal ion affects the biological activity, we have also prepared two triphenyltin(IV) complexes with indomethacin and racemic flurbiprofen (corresponding carboxylate anions), namely $[Ph_3Sn(IND)]$ and $[Ph_3Sn(FBP)]$ (Figure 1). The two compounds have been previously reported [57,58]. In this study, however, these complexes were synthesized using different precursors; furthermore, a single crystal structure analysis of $[Ph_3Sn(IND)]$ is reported and the biological activity of both triphenyltin(IV) complexes was evaluated towards four cell lines of human breast carcinoma, namely BT-474, MCF-7, MDA-MB-468, and HCC1937, using colorimetric MTT- and CV-based cell viability assays.

Furthermore, flow cytometry has been employed in order to understand the mechanism of the drug-induced cytotoxicity.

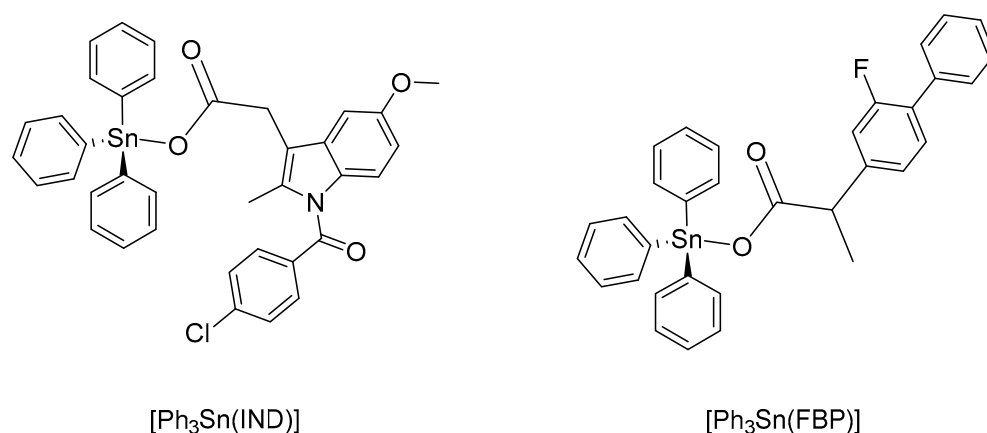


Figure 1. Organotin(IV) carboxylates: triphenyltin(IV) indomethacinate, [Ph₃Sn(IND)], and triphenyltin(IV) flurbiprofenate, [Ph₃Sn(FBP)].

2. Materials and Methods

Reactions were performed implementing standard Schlenk techniques to ensure nitrogen atmosphere. Chemicals (triphenyltin(IV) chloride (Sigma-Aldrich Chemie GmbH, Steinheim, Germany), indomethacin (TCI), and racemic flurbiprofen (Biozol)) were used as purchased. Triethylamine was distilled from KOH and kept over 4 Å molecular sieves previously activated at 150 °C. Toluene was obtained from an MBraun Solvent Purification System (MBraun SPS-800) and kept over 4 Å active molecular sieves. A Heraeus VARIO EL oven was used for carrying out elemental analyses. NMR spectra were recorded on a Bruker AVANCE DRX 400 spectrometer. Tetramethylsilane (TMS) was used as internal standard to reference the NMR spectra; chemical shifts are reported in parts per million; ¹H (400.13 MHz), ¹³C (100.61 MHz) and ¹¹⁹Sn (149.21 MHz). Mass spectra (HR-ESI-MS) were obtained with an FT-ICR-MS Bruker Daltonics ESI mass spectrometer (APEX II, 7 T). X-ray data from single crystals were collected with a Gemini-CCD diffractometer (Rigaku Oxford Diffraction, Oxford, UK).

2.1. Synthesis and Stability of Complexes

A stoichiometric amount of indomethacin or racemic flurbiprofen (0.45 g or 0.32 g, respectively), dissolved in 10 mL toluene, was added to a solution of Ph₃SnCl (0.5 g, 1.3 mmol) in 10 mL toluene. After 20 min stirring, NEt₃ (0.18 mL, 1.3 mmol, 1 eq.) was slowly (10 min) added to the solution and the resulting solution was stirred at room temperature overnight. The formed precipitate, (Et₃NH)Cl, was filtered off. The solvent was evaporated and the solid residue was recrystallized from a 3:1 mixture of chloroform and methanol. For detailed characterization (multinuclear NMR, X-ray crystallographic data and HR-ESI-MS), see SI, Figures S1–S10. Spectroscopic data of [Ph₃Sn(IND)] and [Ph₃Sn(FBP)] are in agreement with those previously reported [57,58].

[Ph₃Sn(IND)]: White solid; yield: 0.76 g (83%). Anal. calcd. for C₃₇H₃₀ClNO₄Sn: C, 62.88; H, 4.28; N, 1.98%. Found: C, 62.46; H, 4.18; N, 1.93%.

[Ph₃Sn(FBP)]: White solid; yield: 0.69 g (88%). Anal. calcd. for C₃₃H₂₇FO₂Sn: C, 66.81; H, 4.59%. Found: C, 66.55; H, 4.29%.

Stability of complexes [Ph₃Sn(IND)] and [Ph₃Sn(FBP)] was evaluated in water-containing DMSO, employing time-resolved (0, 1, 3, 6, 12, 24, 48 and 72 h) ¹H NMR spectroscopy.

2.2. Data Collection and Structure Refinement of [Ph₃Sn(IND)]

The X-ray data from a single crystal of [Ph₃Sn(IND)] were collected with a Gemini-CCD diffractometer (Rigaku Oxford Diffraction, Oxford, UK) employing ω-scan rotation

and Mo-K α radiation ($\lambda = 0.71073 \text{ \AA}$). Data reduction and empirical absorption correction were carried out using CrysAlisPro [62] with SCALE3 ABSPACK program for the later. For solving the structure, SHELXT-2018 [63] with dual-space method were employed, while structure refinement was performed with SHELXL-2018 [64] using full-matrix least-squares routines against F^2 . Anisotropic refinement was carried out for all non-hydrogen atoms, whereas hydrogen atoms were calculated on idealized positions. The C₁₉H₁₅ClNO₄ substituent is disordered on two positions with a ratio of 0.814(5):0.186(5). All chloroform solvent molecules are disordered as well. DIAMOND-4 [65] was used to generate all structural figures. Crystallographic details are listed in Table S1 in the SI.

2.3. In Vitro Studies

The four cell lines of human breast carcinoma utilized in this study were acquired from ATCC, Manassas, USA. Cell viability assays (MTT (3-(4,5-dimethylthiazol-2-yl)-2,5-diphenyltetrazolium bromide) and CV (crystal violet)) were bought from Sigma-Aldrich, Taufkirchen, Germany. Multi-well plates, culture flasks and additional plastics for cell culturing were bought from TPP, Trasadingen, Switzerland and Greiner Bio-One GmbH, Frickenhausen, Germany. Fetal calf serum (FCS), RPMI cell culturing medium, L-glutamine, trypsin/ethylenediaminetetraacetic acid (EDTA) and phosphate-buffered saline (PBS) were all obtained from Capricorn Scientific GmbH, Ebsdorfergrund, Germany. The reagents for fluorescence-activated cell sorting (FACS) were obtained from several suppliers: Thermo Fisher Scientific: annexin V/propidium iodide (AnnV/PI) and 4-amino-5-methylamino-2',7'-difluorofluorescein diacetate (DAF-FM); BD horizon: dihydrorhodamine (DHR) and carboxyfluorescein succinimidyl (CFSE); Sigma Aldrich: acridine orange (AO) and 4',6-diamidino-2-phenylindole (DAPI); R & D scientific: ApoStat.

2.4. Cell Lines, General Conditions and IC₅₀ Determination

Cytotoxic effects of the NSAIDs used as ligands, indomethacin and flurbiprofen, and organotin(IV) compounds [Ph₃Sn(IND)] and [Ph₃Sn(FBP)] were evaluated using colorimetric MTT- and CV-based cell viability assays against four cell lines from different human breast carcinoma. BT-474 and MCF-7 are estrogen-positive cells, while MDA-MB-468 and HCC1937 are triple-negative cells [66]. Cells' cultivation was carried out in T-75 flasks using RPMI 1640 medium supplied with 10% FCS inactivated by heat, L-glutamine (2 mM) and 1% penicillin/streptomycin, at 37 °C, in a humidified environment with 5% CO₂ until subconfluency ~ 80% was reached. Cell passaging and seeding was carried out after washing of adherent cells using PBS and detaching them applying trypsin/EDTA solution (0.05%) in PBS.

Utilizing the aforementioned cell growth medium, cells were seeded in plates with 96 wells, at a 6000/100 μL /well density. Before treatment with the investigated compounds, cells were given 24 h to adhere. Stock solutions of cisplatin, indomethacin, flurbiprofen, [Ph₃Sn(IND)], and [Ph₃Sn(FBP)] were made in DMSO and subsequently diluted in growth medium to reach the following concentrations: 300, 100, 30, 10, 3, 1, and 0.1 μM for cisplatin, 100, 50, 25, 12.5, 6.25, 3.125, and 1.6 μM for the NSAIDs and 10, 5, 1, 0.5, 0.1, 0.01, and 0.001 μM for [Ph₃Sn(IND)] and [Ph₃Sn(FBP)]. A positive control of digitonin (100 μM) was included in each 96-well plate. Three independent biological replicates and four technical replicates were conducted. After 72 h treatment, cell viability was assessed. For the MTT assay, cells were initially rinsed with PBS and then exposed for 1 h to the working solution containing 0.5 mg mL^{-1} MTT in culture medium. The MTT solution was then removed, the formazan formed was dissolved in DMSO and its absorbance was measured at 570 nm and 670 nm employing a multi-well plate reader SpectraMax M5 (Molecular Devices, San Jose, CA, USA). For the CV assay, cells were first washed with PBS, fixated with 4% paraformaldehyde (PFA), dried after removal of the PFA solution and only then stained for 20 min with a 10% crystal violet solution. After discarding the staining solution, stained cells were supplied with acetic acid (33% in aqua bidest.) and the absorbance was recorded by using the previously described method at the same wavelengths [67]. Cell viability is

expressed as a percentage of untreated cells with the mean value being computed using a four-parametric logistic function [68]. SigmaPlot 14.0 and Microsoft Excel 2013 programs were used for data analysis and IC₅₀ value calculation.

2.5. Flow Cytometry

BT-474 cells were seeded in 6-well plates, with a density of 150,000 cells/well. Cells were allowed to adhere overnight, after which they were treated with IC₅₀ value concentrations of [Ph₃Sn(IND)], [Ph₃Sn(FBP)] and cisplatin and subjected to flow cytometry (BD FACSAria III) assessment. For that, several staining procedures were employed including (1) AnnV/PI to identify cells undergoing apoptosis, (2) ApoStat to detect caspase activity, (3) AO to monitor autophagy induction, (4) DHR to measure reactive oxygen species/reactive nitrogen species (ROS/RNS), (5) DAF-FM to detect intracellular NO, and (6) CFSE to track the impact on cellular proliferation.

AnnV/PI, ApoStat, AO and DAF-FM staining was carried out according to the manufacturer's recommendations after 48-h-long exposure to the examined compounds, trypsinization and washing with PBS. AnnV/PI (5% AnnV, 2% PI in PBS) [69] and AO (1 µg mL⁻¹ PBS) staining solutions were applied for 15 min at room temperature or at 37 °C, respectively, in an environment with 5% CO₂. For caspase activity determination, 30 min exposure to the ApoStat (1% ApoStat, 5% FCS in PBS) stain at 37 °C with 5% CO₂ was applied. For NO production analysis, cells were dyed with DAF-FM dye (5 µM DAF-FM, 10% FCS in RPMI) for 1 h at 37 °C with 5% CO₂. To neutralize the stain, the cells were incubated in serum-free medium for 15 min. Finally, cells' detachment was performed and flow cytometry examination was conducted through measurement of fluorescein isothiocyanate (FITC) fluorescence.

For ROS/RNS production analysis and cell proliferation investigations, cells were first dyed with the appropriate stain solution before being subjected to 48 h treatment with the experimental agents and cisplatin. DHR (1 µM DHR, 0.1% FCS in PBS) and CFSE (1 µM CFSE, 0.1% FCS in PBS) [70] stains were applied overnight at 37 °C with 5% CO₂. After dyeing and 48 h treatment, trypsin-EDTA was used to detach the cells, which were subsequently rinsed with PBS and finally analyzed by flow cytometry.

3. Results and Discussion

3.1. Synthesis, Characterization, and Stability of Organotin(IV) Carboxylates

The two organotin(IV) complexes, triphenyltin(IV) indomethacinate [Ph₃Sn(IND)], and triphenyltin(IV) flurbiprofenate [Ph₃Sn(FBP)], were prepared in a reaction of the corresponding NSAID (HIND or HFBP) deprotonated with NEt₃ and an equimolar amount of Ph₃SnCl. The preparation of both organotin(IV) compounds, starting from triphenyltin(IV) chloride, resulted in higher yields and easier purification of the obtained compounds than previously reported procedures involving Ph₃SnOH as starting material [57,58]. Elemental analysis was employed to verify purity of the produced complexes. Further characterization of the compounds was also carried out by multinuclear NMR spectroscopy (¹H, ¹³C, ¹¹⁹Sn) and mass spectrometry. The obtained results, presented in the SI (Figures S1–S10), are in agreement with the reported ones [57,58].

The complexes [Ph₃Sn(IND)] and [Ph₃Sn(FBP)] are stable in water-containing DMSO solution during a 72-h period, as shown by time-resolved ¹H NMR spectroscopy. No ligand exchange or complex degradation was observed during this time (Figures S11 and S12).

Single crystals adequate for X-ray diffraction studies were formed slowly diffusing methanol into a CHCl₃ solution of [Ph₃Sn(IND)]. [Ph₃Sn(IND)] crystallizes with sixteen monomeric units per unit cell, in the tetragonal space group *I*₄¹/*a*. The trigonal-planar SnPh₃ moieties are connected by bridging carboxylato ligands in the axial positions (Figure 2) forming polymeric helical chains (Figure 3). Consequently, with equatorial phenyl groups and two axial oxygen atoms belonging to two distinct carboxylato (IND) ligands, the penta-coordinated central tin atom displays an almost perfect trigonal bipyramidal geometry. Thus, the C–Sn1–O, C–Sn1–C (C20–Sn1–C26, C20–Sn1–C32 and C26–Sn1–C32), and O1–Sn–O2'

angles are close to 90, 120 and 180°, respectively. The Sn–O (Sn1–O1 2.182(7), Sn1–O2' 2.274(7) Å) and Sn–C bond lengths (Sn1–C26 2.108(5), Sn1–C20 2.129(5), Sn1–C32 2.129(5) Å) are comparable to ones reported for analogous triorganotin(IV) carboxylate complexes [71–76]. The carboxylato ligand bridges two tin atoms which are symmetry-independent resulting in distinct Sn–O bond lengths (Table 1).

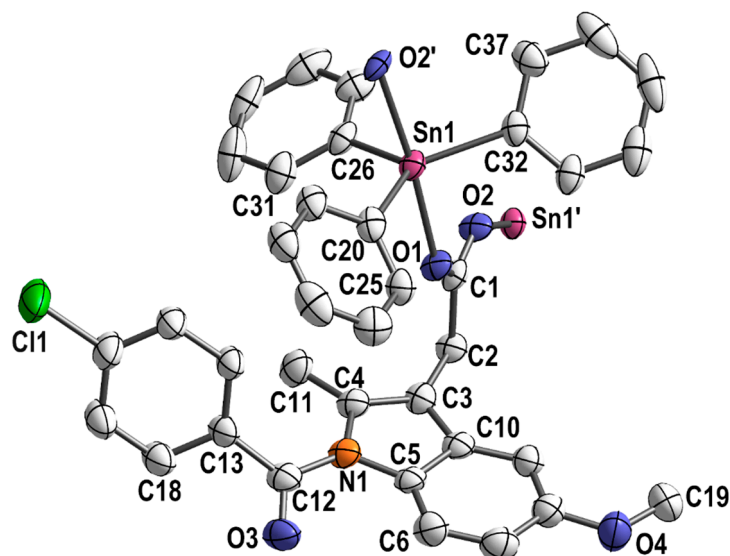


Figure 2. Section of the polymeric structure of $[\text{Ph}_3\text{Sn}(\text{IND})]$; hydrogen atoms and solvent molecules are omitted for clarity; thermal ellipsoids are set at 50% probability level.

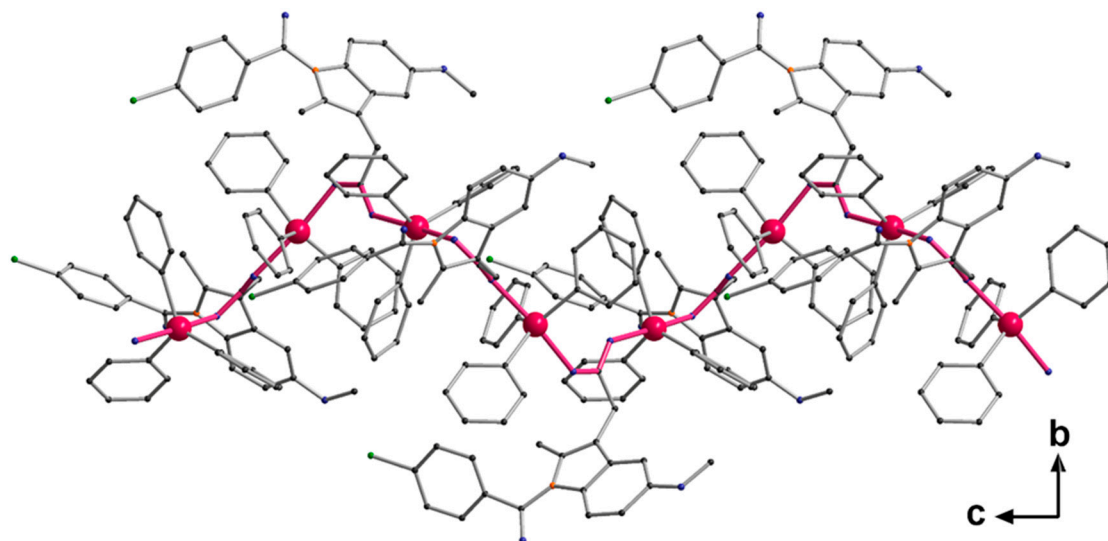


Figure 3. Helical chain structure of $[\text{Ph}_3\text{Sn}(\text{IND})]$, propagation via $\text{O} \rightarrow \text{Sn}$ coordination. Bonds forming the basis of the helix are highlighted in pink.

Table 1. Selected Bond Lengths [Å] and Angles [°] for $[\text{Ph}_3\text{Sn}(\text{IND})]$.

Bond Lengths [Å]		Bond Angles [°]	
Sn1–O1	2.182(7)	C20–Sn1–C26	116.1(2)
Sn1–O2'	2.274(7)	C26–Sn1–C32	121.1(2)
Sn1–C26	2.108(5)	C20–Sn1–C32	122.7(2)
Sn1–C20	2.129(5)	C–Sn1–O	83.9(2) to 95.3(3)
Sn1–C32	2.129(5)	O1–Sn1–O2'	174.6(5)
symmetry operation $' -y + 3/4, x + 1/4, z + 1/4$			

3.2. Cytotoxic Activity

Following a 72 h treatment, the in vitro cytotoxicity of [Ph₃Sn(IND)] and [Ph₃Sn(FBP)] was evaluated in a variety of breast carcinoma cells, namely triple-positive (ER+,PR+,HER2+) BT-474 causing invasive ductal breast cancer, COX-1 expressing MCF-7 (ER+,PR+,HER2-), COX-2 expressing MDA-MB-468 (ER-,PR-,HER2-), and HCC1937 cancer cells with BRCA1 mutation (ER-,PR-,HER2-). Investigations were made with two distinct cell viability assays, MTT and CV. MTT is an indirect method for cell viability determination which utilizes the capacity of living cells to catalyze tetrazolium salt reduction in MTT to formazan [77]. This is the result of mitochondrial dehydrogenase activity taking place in the mitochondria of viable cells. Consequently, substances that alter cellular metabolism through elevation of the level of reduced nicotinamide adenine dinucleotide phosphate (NADPH) or the activity of lactate dehydrogenase (LDH) may have a considerable impact on the results of the MTT experiment [78–81]. Therefore, for higher reliability of the results, also the direct, non-enzymatic CV assay was employed. The cytotoxicity of the organotin(IV) complexes was compared to that of the two NSAIDs utilized as ligands, indomethacin and flurbiprofen, as well as cisplatin which is used as standard clinical therapy. The decrease in cell viability in the selected cell lines upon treatment with increasing concentrations of [Ph₃Sn(IND)], [Ph₃Sn(FBP)] and cisplatin determined by MTT and CV assays is presented in the SI (Figures S13–S16). The IC₅₀ values are reported in Table 2.

Table 2. IC₅₀ values (mean ± SD, [μM]) of synthesized complexes and cisplatin obtained with MTT and CV assays after 72 h treatment. IC₅₀ values of the ligand precursors, indomethacin and flurbiprofen, are >100 μM as found by both MTT and CV assays after 72 h treatment.

		MDA-MB-468	HCC1937	MCF-7	BT-474
		IC ₅₀ [μM]			
[Ph ₃ Sn(IND)]	MTT	0.11 ± 0.03	0.15 ± 0.01	0.13 ± 0.02	0.10 ± 0.02
	CV	0.14 ± 0.02	0.20 ± 0.02	0.17 ± 0.01	0.15 ± 0.02
[Ph ₃ Sn(FBP)]	MTT	0.11 ± 0.01	0.13 ± 0.01	0.12 ± 0.03	0.076 ± 0.003
	CV	0.12 ± 0.02	0.17 ± 0.01	0.16 ± 0.01	0.16 ± 0.01
Cisplatin	MTT	0.60 ± 0.11	4.26 ± 0.73	32.00 ± 4.29	70.30 ± 8.45
	CV	3.32 ± 0.19	7.62 ± 0.90	33.59 ± 4.83	54.86 ± 6.03

As expected, none of the four tumor cell lines was susceptible to the COX inhibitors alone (>100 μM). The cytotoxic potential of both organotin(IV) carboxylates, on the contrary, was significantly higher compared to cisplatin's activity, exhibiting nanomolar IC₅₀ values in all cases. Both complexes [Ph₃Sn(IND)] and [Ph₃Sn(FBP)] had a comparable effect on all four cell lines. With regard to cisplatin, their activity was much higher, resulting in at least 24 times lower IC₅₀ values towards the MDA-MB-468 cell line and up to 366 times lower IC₅₀ values towards the BT-474 cell line. Similarly high activity was previously proven for [Ph₃Sn(IND)] against HeLa cervical cancer cells and SKLU-1 lung adenocarcinoma cells [57]. The investigated complexes showed much higher activity with respect to the structurally similar complex with an ibuprofenate ligand ([Ph₃Sn(IBF)]) which has been found to be active against the Caco-2 colorectal adenocarcinoma cell line, but only remotely active or completely inactive against the DU145 (prostate carcinoma) cells and the HCT-15 (colon adenocarcinoma) cells, respectively [55]. In our previous study, flurbiprofen was used as an axial ligand of a cisplatin-based platinum(IV) conjugate and the cytotoxic activity of this *cis,trans,cis*-[PtCl₂(FBP)₂(NH₃)₂] complex was assessed against the same four breast carcinoma cell lines used in the present study [61]. The obtained results show very similar cytotoxic activity for [Ph₃Sn(FBP)] and the cisplatin-flurbiprofenate complex suggesting that both NSAID-metal complexes with tin(IV) and platinum(IV) are highly active. Since the COX inhibitory potential of the prepared metal complexes was not assessed in these studies, the mechanism underlying the increase in cytotoxic efficacy following NSAID conjugation is unclear. The findings from the CV and MTT assays for [Ph₃Sn(IND)] and

[Ph₃Sn(FBP)] are in very good agreement with each other, while for cisplatin towards the BT-474, HCC1937 and MDA-MB-468 cells, some discrepancies were identified. This suggests that the investigated organotin(IV) carboxylates have different mechanism of action than cisplatin, not affecting the cell metabolism pathways.

3.3. Mode of Cytotoxic Activity

Flow cytometry was employed in order to comprehend the mechanism underlying the drug-induced cytotoxicity. In this method, a specific type of cell in a heterogeneous environment is recognized and physically separated using fluorescently labeled target-specific antibodies. This enables analysis of the nucleic acid material, presence of characteristic proteins, as well as phenotype-specific metabolic content and, therefore, valuable information on cell proliferation, apoptosis and autophagy, ROS/RNS, and NO production, etc., can be acquired. These data allow for conclusions regarding the drug's mechanism of action to be drawn. In the present investigation, BT-474 cells underwent treatment with IC₅₀ doses of [Ph₃Sn(IND)], [Ph₃Sn(FBP)] and cisplatin before undergoing a variety of FACS assessments. This cell line was chosen for the mechanistic studies because of the high cytotoxicity of the investigated compounds against it, which is also the greatest advancement in comparison to cisplatin.

In order to determine whether [Ph₃Sn(IND)] and [Ph₃Sn(FBP)] induce apoptotic cell death, AnnV/PI staining was used. This method relies on the relocation of the membrane phospholipid phosphatidylserine (PS) from the internal to the external side of the membrane, causing a change of the plasma membrane asymmetry, which is a key hallmark of apoptosis. Because of its strong affinity for PS, the annexin V dye acts as a sensor for cells undergoing apoptosis including early apoptotic cells [82]. As the apoptotic process progresses, the intactness of the membrane is lost and it becomes permeable for the second dye, PI. Therefore, cells that are both AnnV- and PI-positive, are in late apoptosis or dead already. Results presented in Figure 4 show that after 48 h treatment with [Ph₃Sn(IND)] and [Ph₃Sn(FBP)], an apoptotic process is not yet ongoing and the number of surviving cells is not significantly influenced, while cisplatin treatment leads to a slight elevation of late apoptotic BT-474 cells population.

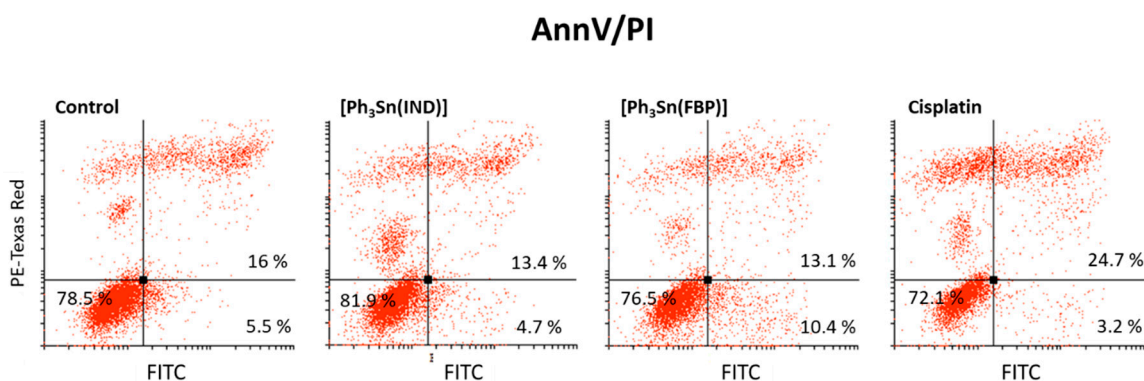


Figure 4. Capacity of organotin(IV) complexes ([Ph₃Sn(IND)] and [Ph₃Sn(FBP)]) and cisplatin to induce apoptotic cell death—early and late apoptotic cells (after 48 h treatment).

Identification of activated caspases is another marker of apoptosis. These cytosolic cysteine proteases are implicated in the onset as well as execution of apoptosis. Therefore, detection of this enzyme's activity indicates the presence of apoptotic cells. This can be probed utilizing the ApoStat assay. Figure 5A reveals that [Ph₃Sn(IND)] and [Ph₃Sn(FBP)] do not activate, but rather inhibit the activity of these enzymes, whereas cisplatin has no effect on the caspase activity, although previous reports link cisplatin-induced cell death with caspase-activated apoptosis [61,83–87]. These results, however, are in agreement with the ones obtained with the AnnV/PI experiments and confirm that apoptotic mechanisms in BT-474 cells could not be detected within the 48 h of treatment.

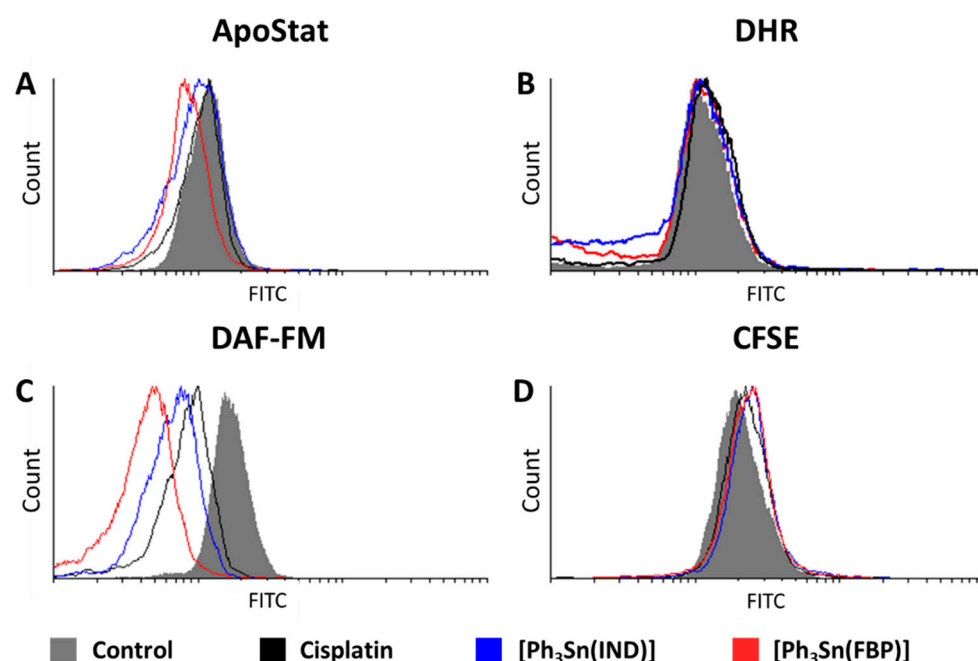


Figure 5. Effect of organotin(IV) complexes ($[\text{Ph}_3\text{Sn}(\text{IND})]$ and $[\text{Ph}_3\text{Sn}(\text{FBP})]$) and cisplatin on BT-474 cells: (A) caspase activation, (B) ROS/RNS production, (C) NO production, and (D) cell proliferation potential.

Lack of impact was also the outcome of the DHR staining investigation conducted with the aim to assess the influence of $[\text{Ph}_3\text{Sn}(\text{IND})]$ and $[\text{Ph}_3\text{Sn}(\text{FBP})]$ and cisplatin on the production of ROS and RNS. Although increased ROS/RNS production has been previously related to cytotoxicity brought on by cisplatin [83,88,89] as well as cisplatin-NSAID conjugates [61], in BT-474 cells treated with cisplatin or $[\text{Ph}_3\text{Sn}(\text{IND})]$ and $[\text{Ph}_3\text{Sn}(\text{FBP})]$, only slightly elevated ROS/RNS production could be detected (Figure 5B). Thus, on breast BT-474 cells the tested complexes did not induce cell death by orchestrating antioxidant systems [90].

Interestingly, all three compounds have a most prominent effect on the generation of nitric oxide resulting in a significant decrease in NO. This effect, as displayed in Figure 5C, is most pronounced for the tin(IV)-based compounds with $[\text{Ph}_3\text{Sn}(\text{FBP})]$ being the more potent NO suppressor, while cisplatin causes the least notable inhibition. Nitric oxide is a bioactive molecule having a profound impact on numerous physiological and pathological processes [91]. In cancer biology, the role of NO is controversial as it can exert both carcinogenic or anticancer effects, depending on the location, time, and its concentration [92–95]. NO is produced enzymatically from nitric oxide synthase (NOS). Despite the existence of three isoforms of this enzyme (neuronal, inducible, and endothelial), the inducible form (iNOS) has the most compelling association with tumor progression and metastasis [92]. Namely, elevated iNOS expression has been reported for different cancers [96–99], including breast cancer [100–103], where iNOS overexpression has been linked with tumor aggressiveness and poor prognosis for the patients. Furthermore, Chang et al. [104] have shown that treatment with iNOS inhibitors can suppress tumor cell proliferation as well as cancer stem cells' capacity for self-renewal and migration, hence lowering tumor initiation, growth, and the incidence of lung metastases from breast cancer. Considering the fact that our findings suggest that the metal complexes cause inhibition of cell proliferation (evaluated with a CFSE assay; Figure 5D) in BT 474 cells, it can be assumed that the suppression of NO production correlates to reduced cell proliferation, possibly through decreasing iNOS gene expression. A previous study reports that flurbiprofen has the ability to inhibit iNOS expression in RAW 264.7 macrophages [105]. Furthermore, indomethacin has been found to decrease iNOS gene expression and reduce tumor growth in vivo in breast tumor-bearing

mice [106]. These findings regarding our ligand precursors, indomethacin and flurbiprofen, further corroborate our conclusions that the cytotoxic capacity of $[\text{Ph}_3\text{Sn}(\text{IND})]$ and $[\text{Ph}_3\text{Sn}(\text{FBP})]$ could be due to iNOS suppression-mediated reduction in NO production.

Finally, an acridine orange (AO) assay was used to investigate if $[\text{Ph}_3\text{Sn}(\text{IND})]$ and $[\text{Ph}_3\text{Sn}(\text{FBP})]$ as well as cisplatin can trigger autophagy in BT-474 cells. This controlled lysosomal mechanism is engaged in the breakdown and reuse of cytoplasmic components. Amino and fatty acids, which are being created during this process, can be utilized to produce proteins or energy, which are critical for a cell's ability to survive in a starvation situation. However, autophagy can also result in cell death upon exposure to chemical therapy [107]. According to our findings (Figure 6), cisplatin, $[\text{Ph}_3\text{Sn}(\text{IND})]$ and $[\text{Ph}_3\text{Sn}(\text{FBP})]$ did not have any significant influence on autophagy after 48 h treatment, thus neither cytoprotective nor cytotoxic effect of autophagy [108] can be expected upon treatment of B-474 cells with the investigated complexes.

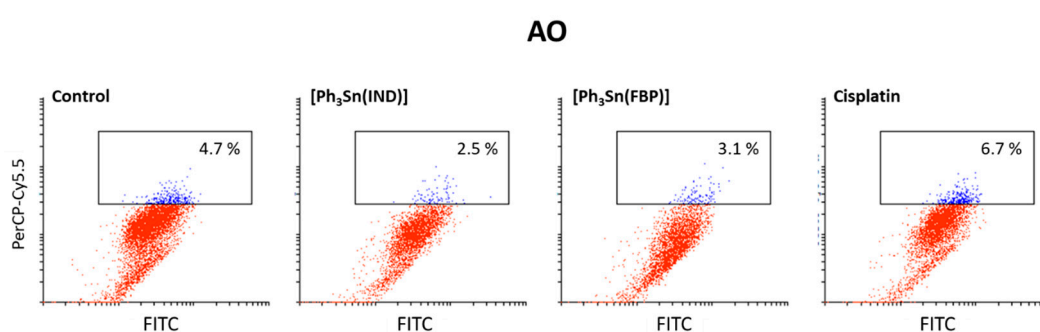


Figure 6. Autophagy induction in BT-474 cells upon 48 h treatment with organotin(IV) complexes ($[\text{Ph}_3\text{Sn}(\text{IND})]$ and $[\text{Ph}_3\text{Sn}(\text{FBP})]$) and cisplatin.

4. Conclusions

In this study, two triphenyltin(IV) carboxylates with NSAIDs as ligands, $[\text{Ph}_3\text{Sn}(\text{IND})]$ and $[\text{Ph}_3\text{Sn}(\text{FBP})]$, were prepared and evaluated for their *in vitro* antiproliferative effect towards four different cell lines of breast carcinoma. The ligand precursors, indomethacin and flurbiprofen, exhibited no impact on the examined cancer cells' proliferation. On the other hand, the organotin(IV) complexes demonstrated IC_{50} values at nanomolar concentrations in the range of 0.076–0.200 μM . This superior cytotoxicity, demonstrated against all cell lines involved, represents a significant enhancement in comparison to the effect of cisplatin. Various biological experiments used to investigate these compounds' mode of action suggested that neither apoptotic nor autophagy mechanisms were activated within the 48 h treatment. However, slightly elevated ROS/RNS production as well as inhibition of the cell proliferation were confirmed for these compounds; the latter might be related to the massive suppression of NO production. Gene expression experiments could be additionally performed to evaluate if the extensive NO production suppression is caused by inhibition of iNOS expression.

Supplementary Materials: The following supporting information can be downloaded at: <https://www.mdpi.com/article/10.3390/biom13040595/s1>, Figure S1: ^1H NMR spectrum of $[\text{Ph}_3\text{Sn}(\text{IND})]$ in CDCl_3 ; Figure S2: $^{13}\text{C}\{^1\text{H}\}$ NMR spectrum of $[\text{Ph}_3\text{Sn}(\text{IND})]$ in CDCl_3 ; Figure S3: $^{119}\text{Sn}\{^1\text{H}\}$ NMR spectrum of $[\text{Ph}_3\text{Sn}(\text{IND})]$ in CDCl_3 ; Figures S4 and S5: HR-ESI-MS of $[\text{Ph}_3\text{Sn}(\text{IND})]$ (positive mode, CH_3OH); Figure S6: ^1H NMR spectrum of $[\text{Ph}_3\text{Sn}(\text{FBP})]$ in CDCl_3 ; Figure S7: $^{13}\text{C}\{^1\text{H}\}$ NMR spectrum of $[\text{Ph}_3\text{Sn}(\text{FBP})]$ in CDCl_3 ; Figure S8: $^{119}\text{Sn}\{^1\text{H}\}$ NMR spectrum of $[\text{Ph}_3\text{Sn}(\text{FBP})]$ in CDCl_3 ; Figures S9 and S10: HR-ESI-MS of $[\text{Ph}_3\text{Sn}(\text{FBP})]$ (positive mode, CH_3OH); Figure S11: Stability of $[\text{Ph}_3\text{Sn}(\text{IND})]_2$ in DMSO-d_6 over 72 h; time-resolved ^1H NMR spectra; Figure S12: Stability of $[\text{Ph}_3\text{Sn}(\text{FBP})]_2$ in DMSO-d_6 over 72 h; time-resolved ^1H NMR spectra; Figure S13: Cell viability of $[\text{Ph}_3\text{Sn}(\text{IND})]$, $[\text{Ph}_3\text{Sn}(\text{FBP})]$ and cisplatin determined by MTT and CV assays in MDA-MB-468 breast cancer cell line; Figure S14: Cell viability of $[\text{Ph}_3\text{Sn}(\text{IND})]$, $[\text{Ph}_3\text{Sn}(\text{FBP})]$ and cisplatin determined by MTT and CV assays in HCC1937 breast cancer cell line; Figure S15: Cell viability of $[\text{Ph}_3\text{Sn}(\text{IND})]$,

[Ph₃Sn(FBP)] and cisplatin determined by MTT and CV assays in MCF-7 breast cancer cell line; Figure S16: Cell viability of [Ph₃Sn(IND)], [Ph₃Sn(FBP)] and cisplatin determined by MTT and CV assays in BT-474 breast cancer cell line; Table S1: Crystal data and structure refinement of [Ph₃Sn(IND)].

Author Contributions: I.P., G.N.K. and E.H.-H. conceptualized the project. I.P., M.S., I.M. and P.L. did investigation, formal analysis of data and data curation. I.P. wrote the original draft. G.N.K. and E.H.-H. supervised the work, reviewed, and edited the original draft, acquired the funding, and administrated the project. All authors have read and agreed to the published version of the manuscript.

Funding: This work was financially supported through the program FEM POWER (funded by the operational program ESF Saxony-Anhalt WISSENSCHAFT Chancengleichheit with funds from the European Union; doctoral grant for I.P.), the Graduate School “Building with Molecules and Nanoobjects (BuildMoNa)” and the Research Academy Leipzig.

Institutional Review Board Statement: Not applicable.

Informed Consent Statement: Not applicable.

Data Availability Statement: Data is contained within the article or supplementary material.

Conflicts of Interest: The authors declare no conflict of interest.

References

1. Bray, F.; Laversanne, M.; Weiderpass, E.; Soerjomataram, I. The ever-increasing importance of cancer as a leading cause of premature death worldwide. *Cancer* **2021**, *127*, 3029–3030. [[CrossRef](#)] [[PubMed](#)]
2. Sung, H.; Ferlay, J.; Siegel, R.L.; Laversanne, M.; Soerjomataram, I.; Jemal, A.; Bray, F. Global cancer statistics 2020: GLOBOCAN estimates of incidence and mortality worldwide for 36 cancers in 185 countries. *CA Cancer J. Clin.* **2021**, *71*, 209–249. [[CrossRef](#)] [[PubMed](#)]
3. Hawash, M. Recent advances of tubulin inhibitors targeting the colchicine binding site for cancer therapy. *Biomolecules* **2022**, *12*, 1843. [[CrossRef](#)] [[PubMed](#)]
4. Arnesano, F.; Natile, G. Mechanistic insight into the cellular uptake and processing of cisplatin 30 years after its approval by FDA. *Coord. Chem. Rev.* **2009**, *253*, 2070–2081. [[CrossRef](#)]
5. Higby, D.J.; Higby, D.J.; Wallace, H.J., Jr.; Albert, D.J.; Holland, J.F. Diaminodichloroplatinum: A phase I study showing responses in testicular and other tumors. *Cancer* **1974**, *33*, 1219–1225. [[CrossRef](#)]
6. Jamieson, E.R.; Lippard, S.J. Structure, recognition, and processing of cisplatin-DNA adducts. *Chem. Rev.* **1999**, *99*, 2467–2498. [[CrossRef](#)] [[PubMed](#)]
7. Dilruba, S.; Kalayda, G.V. Platinum-based drugs: Past, present and future. *Cancer Chemother. Pharmacol.* **2016**, *77*, 1103–1124. [[CrossRef](#)] [[PubMed](#)]
8. Johnstone, T.C.; Suntharalingam, K.; Lippard, S.J. The next generation of platinum drugs: Targeted Pt(II) agents, nanoparticle delivery, and Pt(IV) prodrugs. *Chem. Rev.* **2016**, *116*, 3436–3486. [[CrossRef](#)]
9. Kenny, R.G.; Marmion, C.J. Toward multi-targeted platinum and ruthenium drugs—A new paradigm in cancer drug treatment regimens? *Chem. Rev.* **2019**, *119*, 1058–1137. [[CrossRef](#)]
10. Wang, D.; Lippard, S.J. Cellular processing of platinum anticancer drugs. *Nat. Rev. Drug Discov.* **2005**, *4*, 307–320. [[CrossRef](#)]
11. Oun, R.; Moussa, Y.E.; Wheate, N.J. The side effects of platinum-based chemotherapy drugs: A review for chemists. *Dalton Trans.* **2018**, *47*, 6645–6653. [[CrossRef](#)]
12. Simpson, P.V.; Desai, N.M.; Casari, I.; Massi, M.; Falasca, M. Metal-based antitumor compounds: Beyond cisplatin. *Future Med. Chem.* **2019**, *11*, 119–135. [[CrossRef](#)] [[PubMed](#)]
13. Banti, C.N.; Hadjikakou, S.K.; Sismanoglu, T.; Hadjiliadis, N. Anti-proliferative and antitumor activity of organotin(IV) compounds. An overview of the last decade and future perspectives. *J. Inorg. Biochem.* **2019**, *194*, 114–152. [[CrossRef](#)] [[PubMed](#)]
14. Chen, Z.-F.; Orvig, C.; Liang, H. Multi-target metal-based anticancer agents. *Curr. Top. Med. Chem.* **2017**, *17*, 3131–3145. [[CrossRef](#)]
15. Gómez-Ruiz, S.; Maksimović-Ivanić, D.; Mijatović, S.; Kaluderović, G.N. On the discovery, biological effects, and use of cisplatin and metallocenes in anticancer chemotherapy. *Bioinorg. Chem. Appl.* **2012**, *2012*, 140284. [[CrossRef](#)] [[PubMed](#)]
16. Almodares, Z.; Lucas, S.J.; Crossley, B.D.; Basri, A.M.; Pask, C.M.; Hebden, A.J.; Phillips, R.M.; McGowan, P.C. Rhodium, iridium, and ruthenium half-sandwich picolinamide complexes as anticancer agents. *Inorg. Chem.* **2014**, *53*, 727–736. [[CrossRef](#)]
17. Alama, A.; Tasso, B.; Novelli, F.; Sparatore, F. Organometallic compounds in oncology: Implications of novel organotin(IV) antitumor agents. *Drug Discov. Today* **2009**, *14*, 500–508. [[CrossRef](#)]
18. Hadi, A.G.; Jawad, K.; Ahmed, D.S.; Yousif, E. Synthesis and biological activities of organotin(IV) carboxylates: A review. *Syst. Rev. Pharm.* **2019**, *10*, 26–31. [[CrossRef](#)]
19. Syed Annuar, S.N.; Kamaludin, N.F.; Awang, N.; Chan, K.M. Cellular basis of organotin(IV) derivatives as anticancer metallodrugs: A review. *Front. Chem.* **2021**, *9*, 657599. [[CrossRef](#)]

20. Esmail, S.A.A.; Shamsi, M.; Chen, T.; Al-asbahy, W.M. Design, synthesis and characterization of tin-based cancer chemotherapy drug entity: In vitro DNA binding, cleavage, induction of cancer cell apoptosis by triggering DNA damage-mediated P53 phosphorylation and molecular docking. *Appl. Organomet. Chem.* **2019**, *33*, e4651. [[CrossRef](#)]
21. Rocamora-Reverte, L.; Carrasco-García, E.; Ceballos-Torres, J.; Prashar, S.; Kaluđerović, G.N.; Ferragut, J.A.; Gómez-Ruiz, S. Study of the anticancer properties of tin(IV) carboxylate complexes on a panel of human tumor cell lines. *ChemMedChem* **2012**, *7*, 301–310. [[CrossRef](#)] [[PubMed](#)]
22. Pellerito, C.; D'Agati, P.; Fiore, T.; Mansueto, C.; Mansueto, V.; Stocco, G.; Nagy, L.; Pellerito, L. Synthesis, structural investigations on organotin(IV) chlorin-e₆ complexes, their effect on sea urchin embryonic development and induced apoptosis. *J. Inorg. Biochem.* **2005**, *99*, 1294–1305. [[CrossRef](#)] [[PubMed](#)]
23. Pellerito, C.; Nagy, L.; Pellerito, L.; Szorcik, A. Biological activity studies on organotin(IV)ⁿ⁺ complexes and parent compounds. *J. Organomet. Chem.* **2006**, *691*, 1733–1747. [[CrossRef](#)]
24. Hadjikakou, S.; Hadjiliadis, N. Antiproliferative and anti-tumor activity of organotin compounds. *Coord. Chem. Rev.* **2009**, *253*, 235–249. [[CrossRef](#)]
25. Xanthopoulou, M.N.; Hadjikakou, S.K.; Hadjiliadis, N.; Schürmann, M.; Jurkschat, K.; Michaelides, A.; Skoulika, S.; Bakas, T.; Binolis, J.; Karkabounas, S.; et al. Synthesis, structural characterization and in vitro cytotoxicity of organotin(IV) derivatives of heterocyclic thioamides, 2-mercaptobenzothiazole, 5-chloro-2-mercaptobenzothiazole, 3-methyl-2-mercaptobenzothiazole and 2-mercaptopicnicotinic acid. *J. Inorg. Biochem.* **2003**, *96*, 425–434. [[CrossRef](#)] [[PubMed](#)]
26. Xanthopoulou, M.N.; Hadjikakou, S.K.; Hadjiliadis, N.; Milaeva, E.R.; Gracheva, J.A.; Tyurin, V.Y.; Kourkoumelis, N.; Christoforidis, K.C.; Metsios, A.K.; Karkabounas, S.; et al. Biological studies of new organotin(IV) complexes of thioamide ligands. *Eur. J. Med. Chem.* **2008**, *43*, 327–335. [[CrossRef](#)]
27. Xanthopoulou, M.N.; Hadjikakou, S.K.; Hadjiliadis, N.; Kubicki, M.; Skoulika, S.; Bakas, T.; Baril, M.; Butler, I.S. Synthesis, structural characterization, and biological studies of six- and five-coordinate organotin(IV) complexes with the thioamides 2-mercaptobenzothiazole, 5-chloro-2-mercaptobenzothiazole, and 2-mercaptobenzoxazole. *Inorg. Chem.* **2007**, *46*, 1187–1195. [[CrossRef](#)] [[PubMed](#)]
28. Xanthopoulou, M.N.; Hadjikakou, S.K.; Hadjiliadis, N.; Kourkoumelis, N.; Milaeva, E.R.; Gracheva, Y.A.; Tyurin, V.Y.; Verginadis, I.; Karkabounas, S.; Baril, M.; et al. Biological studies of organotin(IV) complexes with 2-mercaptopyrimidine. *Russ. Chem. Bull.* **2007**, *56*, 767–773. [[CrossRef](#)]
29. Ma, C.; Jiang, Q.; Zhang, R. Synthesis, properties and crystal structural characterization of diorganotin(IV) derivatives of 2-mercapto-6-nitrobenzothiazole. *Appl. Organomet. Chem.* **2003**, *17*, 623–630. [[CrossRef](#)]
30. Ma, C.; Zhang, J. Syntheses and crystal structures of diorganotin(IV) bis(2-pyridinethiolato-N-oxide) complexes. *Appl. Organomet. Chem.* **2003**, *17*, 788–794. [[CrossRef](#)]
31. Tiekink, E.R.T. Tin dithiocarbamates: Applications and structures. *Appl. Organomet. Chem.* **2008**, *22*, 533–550. [[CrossRef](#)]
32. Saxena, A.K.; Huber, F. Organotin compounds and cancer chemotherapy. *Coord. Chem. Rev.* **1989**, *95*, 109–123. [[CrossRef](#)]
33. Susperregui, J.; Bayle, M.; Lain, G.; Giroud, C.; Baltz, T.; Délérís, G. Synthesis and evaluation of the in vivo trypanocidal activity of water soluble organotin compounds. *Eur. J. Med. Chem.* **1999**, *34*, 617–623. [[CrossRef](#)] [[PubMed](#)]
34. Pellerito, L.; Nagy, L. Organotin(IV)ⁿ⁺ complexes formed with biologically active ligands: Equilibrium and structural studies, and some biological aspects. *Coord. Chem. Rev.* **2002**, *224*, 111–150. [[CrossRef](#)]
35. Basu Baul, T.S.; Rynjah, W.; Rivarola, E.; Lyčka, A.; Holčapek, M.; Jirásko, R.; de Vos, D.; Butcher, R.J.; Linden, A. Synthesis and characterization of bis[dicarboxylatotetraorganodistannoxane] units involving 5-[(E)-2-(Aryl)-1-Diazenyl]-2-hydroxybenzoic acids: An investigation of structures by X-ray diffraction, NMR, electrospray ionisation MS and assessment of in vitro cytotoxicity. *J. Organomet. Chem.* **2006**, *691*, 4850–4862. [[CrossRef](#)]
36. Tian, L.; Sun, Y.; Li, H.; Zheng, X.; Cheng, Y.; Liu, X.; Qian, B. Synthesis, characterization and biological activity of triorganotin 2-phenyl-1,2,3-triazole-4-carboxylates. *J. Inorg. Biochem.* **2005**, *99*, 1646–1652. [[CrossRef](#)] [[PubMed](#)]
37. Han, G.; Yang, P. Synthesis and characterization of water-insoluble and water-soluble dibutyltin(IV) porphinate complexes based on the tris(pyridinyl) porphyrin moiety, their anti-tumor activity in vitro and interaction with DNA. *J. Inorg. Biochem.* **2002**, *91*, 230–236. [[CrossRef](#)] [[PubMed](#)]
38. Gómez-Ruiz, S.; Kaluđerović, G.N.; Prashar, S.; Hey-Hawkins, E.; Erić, A.; Žižak, Ž.; Juranić, Z.D. Study of the cytotoxic activity of di and triphenyltin(IV) carboxylate complexes. *J. Inorg. Biochem.* **2008**, *102*, 2087–2096. [[CrossRef](#)]
39. Tzimopoulos, D.; Sanidas, I.; Varvogli, A.-C.; Czapik, A.; Gdaniec, M.; Nikolakaki, E.; Akrivos, P.D. On the bioreactivity of triorganotin aminobenzoates. Investigation of trialkyl and triarylyltin(IV) esters of 3-amino and 4-aminobenzoic acids. *J. Inorg. Biochem.* **2010**, *104*, 423–430. [[CrossRef](#)]
40. Gielen, M. Review: Organotin compounds and their therapeutic potential: A report from the Organometallic Chemistry Department of the Free University of Brussels. *Appl. Organomet. Chem.* **2002**, *16*, 481–494. [[CrossRef](#)]
41. Gielen, M.; Tiekink, E.R.T. *Metallotherapeutic Drugs and Metal-Based Diagnostic Agents: The Use of Metals in Medicine*; Wiley: New York, NY, USA, 2005.
42. Ghosh, N.; Chaki, R.; Mandal, V.; Mandal, S.C. COX-2 as a target for cancer chemotherapy. *Pharmacol. Rep.* **2010**, *62*, 233–244. [[CrossRef](#)] [[PubMed](#)]
43. Müller-Decker, K.; Fürstenberger, G. The cyclooxygenase-2-mediated prostaglandin signaling is causally related to epithelial carcinogenesis. *Mol. Carcinog.* **2007**, *46*, 705–710. [[CrossRef](#)] [[PubMed](#)]

44. Hawash, M.; Jaradat, N.; Abualhasan, M.; Şüküroğlu, M.K.; Qaoud, M.T.; Kahraman, D.C.; Daraghme, H.; Maslamani, L.; Sawafta, M.; Ratrou, A.; et al. Design, synthesis, molecular docking studies and biological evaluation of thiazole carboxamide derivatives as COX inhibitors. *BMC Chem.* **2023**, *17*, 11. [[CrossRef](#)] [[PubMed](#)]
45. Hawash, M.; Jaradat, N.; Abualhasan, M.; Qaoud, M.T.; Joudeh, Y.; Jaber, Z.; Sawalmeh, M.; Zarour, A.; Mousa, A.; Arar, M. Molecular docking studies and biological evaluation of isoxazole-carboxamide derivatives as COX inhibitors and antimicrobial agents. *3 Biotech* **2022**, *12*, 342. [[CrossRef](#)]
46. Fiori, A.T.M.; Lustrì, W.R.; Magalhães, A.; Corbi, P.P. Chemical, spectroscopic characterization and antibacterial activities in vitro of a novel gold(I)-ibuprofen complex. *Inorg. Chem. Commun.* **2011**, *14*, 738–740. [[CrossRef](#)]
47. Núñez, C.; Fernández-Lodeiro, A.; Fernández-Lodeiro, J.; Carballo, J.; Capelo, J.L.; Lodeiro, C. Synthesis, spectroscopic studies and in vitro antibacterial activity of ibuprofen and its derived metal complexes. *Inorg. Chem. Commun.* **2014**, *45*, 61–65. [[CrossRef](#)]
48. Alves Rico, S.R.; Abbasi, A.Z.; Ribeiro, G.; Ahmed, T.; Wu, X.Y.; de Oliveira Silva, D. Diruthenium(II,III) metallodrugs of ibuprofen and naproxen encapsulated in intravenously injectable polymer-lipid nanoparticles exhibit enhanced activity against breast and prostate cancer cells. *Nanoscale* **2017**, *9*, 10701–10714. [[CrossRef](#)]
49. Kumar, S.; Garg, S.; Sharma, R.P.; Venugopalan, P.; Tenti, L.; Ferretti, V.; Nivellet, L.; Tarpin, M.; Guillon, E. Four monomeric copper(II) complexes of non-steroidal anti-inflammatory drug ibuprofen and N-donor ligands: Syntheses, characterization, crystal structures and cytotoxicity studies. *New J. Chem.* **2017**, *41*, 8253–8262. [[CrossRef](#)]
50. Tabrizi, L.; Chiniforoshan, H.; McArdle, P.; Ebrahimi, M.; Khayamian, T. A novel bioactive Cd(II) polymeric complex with mefenamic acid: Synthesis, crystal structure and biological evaluations. *Inorg. Chim. Acta* **2015**, *432*, 176–184. [[CrossRef](#)]
51. Coyle, B.; McCann, M.; Kavanagh, K.; Devereux, M.; McKee, V.; Kayal, N.; Egan, D.; Deegan, C.; Finn, G.J. Synthesis, X-ray crystal structure, anti-fungal and anti-cancer activity of $[Ag_2(NH_3)_2(salH)_2]$ ($salH_2 = salicylic\ acid$). *J. Inorg. Biochem.* **2004**, *98*, 1361–1366. [[CrossRef](#)]
52. Santos, R.L.S.R.; Bergamo, A.; Sava, G.; de Oliveira Silva, D. Synthesis and characterization of a diruthenium(II,III)-ketoprofen compound and study of the in vitro effects on CRC cells in comparison to the naproxen and ibuprofen derivatives. *Polyhedron* **2012**, *42*, 175–181. [[CrossRef](#)]
53. Rubner, G.; Bendorf, K.; Wellner, A.; Bergemann, S.; Ott, I.; Gust, R. [Cyclopentadienyl]metallocarbonyl complexes of acetylsalicylic acid as neo-anticancer agents. *Eur. J. Med. Chem.* **2010**, *45*, 5157–5163. [[CrossRef](#)] [[PubMed](#)]
54. Dokorou, V.; Primikiri, A.; Kovala-Demertzi, D. The triphenyltin(VI) complexes of NSAIDs and derivatives. Synthesis, crystal structure and antiproliferative activity. Potent anticancer agents. *J. Inorg. Biochem.* **2011**, *105*, 195–201. [[CrossRef](#)] [[PubMed](#)]
55. Kumari, R.; Banerjee, S.; Roy, P.; Nath, M. Organotin(IV) complexes of NSAID, ibuprofen, X-ray structure of $Ph_3Sn(IBF)$, binding and cleavage interaction with DNA and in vitro cytotoxic studies of several organotin complexes of drugs. *Appl. Organomet. Chem.* **2020**, *34*, e5283. [[CrossRef](#)]
56. Pantelić, N.Đ.; Božić, B.; Zmejkovski, B.B.; Banjac, N.R.; Dojčinović, B.; Wessjohann, L.A.; Kaluđerović, G.N. In vitro evaluation of antiproliferative properties of novel organotin(IV) carboxylate compounds with propanoic acid derivatives on a panel of human cancer cell lines. *Molecules* **2021**, *26*, 3199. [[CrossRef](#)]
57. Camacho-Camacho, C.; Rojas-Oviedo, I.; Paz-Sandoval, M.A.; Cárdenas, J.; Toscano, A.; Gielen, M.; Sosa, L.B.; Bártéz, F.S.; Gracia-Mora, I. Synthesis, structural characterization and cytotoxic activity of organotin derivatives of indomethacin. *Appl. Organomet. Chem.* **2008**, *22*, 171–176. [[CrossRef](#)]
58. Mahmood, S.; Ali, S. Synthesis, characterization and biological applications of organotin(IV) derivatives of 2-(2-Fluoro-4-biphenyl)propanoic acid. *Turk. J. Chem.* **2003**, *27*, 657–666.
59. Perou, C.M.; Sørli, T.; Eisen, M.B.; van de Rijn, M.; Jeffrey, S.S.; Rees, C.A.; Pollack, J.R.; Ross, D.T.; Johnsen, H.; Akslen, L.A.; et al. Molecular portraits of human breast tumours. *Nature* **2000**, *406*, 747–752. [[CrossRef](#)]
60. Neumann, W.; Crews, B.C.; Marnett, L.J.; Hey-Hawkins, E. Conjugates of cisplatin and cyclooxygenase inhibitors as potent antitumor agents overcoming cisplatin resistance. *ChemMedChem* **2014**, *9*, 1150–1153. [[CrossRef](#)]
61. Predarska, I.; Saoud, M.; Morgan, I.; Eichhorn, T.; Kaluđerović, G.N.; Hey-Hawkins, E. Cisplatin-cyclooxygenase inhibitor conjugates, free and immobilised in mesoporous silica SBA-15, prove highly potent against triple-negative MDA-MB-468 breast cancer cell line. *Dalton Trans.* **2022**, *51*, 857–869. [[CrossRef](#)]
62. CrysAlisPro data reduction software package. Rigaku Oxford Diffraction: Oxford, UK.
63. Sheldrick, G.M. SHELXT—Integrated space-group and crystal-structure determination. *Acta Crystallogr. A* **2015**, *71*, 3–8. [[CrossRef](#)]
64. Sheldrick, G.M. Crystal structure refinement with Ite SHELXL. *Acta Crystallogr. Sect. C* **2015**, *71*, 3–8. [[CrossRef](#)] [[PubMed](#)]
65. Macrae, C.F.; Bruno, I.J.; Chisholm, J.A.; Edgington, P.R.; McCabe, P.; Pidcock, E.; Rodriguez-Monge, L.; Taylor, R.; van de Streek, J.; Wood, P.A. Mercury CSD 2.0—New features for the visualization and investigation of crystal structures. *J. Appl. Crystallogr.* **2008**, *41*, 466–470. [[CrossRef](#)]
66. Subik, K.; Lee, J.-F.; Baxter, L.; Strzepak, T.; Costello, D.; Crowley, P.; Xing, L.; Hung, M.-C.; Bonfiglio, T.; Hicks, D.G.; et al. The expression patterns of ER, PR, HER2, CK5/6, EGFR, Ki-67 and AR by immunohistochemical analysis in breast cancer cell lines. *Breast Cancer* **2010**, *4*, 35–41. [[CrossRef](#)] [[PubMed](#)]
67. Khan, M.F.; Nasr, F.A.; Noman, O.M.; Alyhya, N.A.; Ali, I.; Saoud, M.; Rennert, R.; Dube, M.; Hussain, W.; Green, I.R.; et al. Cichorins D–F: Three new compounds from *Cichorium intybus* and their biological effects. *Molecules* **2020**, *25*, 4160. [[CrossRef](#)]

68. Drača, D.; Edeler, D.; Saoud, M.; Dojčinović, B.; Dunderović, D.; Đmura, G.; Maksimović-Ivanić, D.; Mijatović, S.; Kaluđerović, G.N. Antitumor potential of cisplatin loaded into SBA-15 mesoporous silica nanoparticles against B16F1 melanoma cells: In vitro and in vivo studies. *J. Inorg. Biochem.* **2021**, *217*, 111383. [[CrossRef](#)]
69. Hawash, M.; Qneibi, M.; Jaradat, N.; Abualhasan, M.; Amer, J.; Amer, E.-H.; Ibraheem, T.; Hindieh, S.; Tarazi, S.; Sobuh, S. The impact of filtered water-pipe smoke on healthy versus cancer cells and their neurodegenerative role on AMPA receptor. *Drug Chem. Toxicol.* **2022**, *45*, 2292–2300. [[CrossRef](#)]
70. Krajnović, T.; Maksimović-Ivanić, D.; Mijatović, S.; Drača, D.; Wolf, K.; Edeler, D.; Wessjohann, L.A.; Kaluđerović, G.N. Drug delivery system for emodin based on mesoporous silica SBA-15. *Nanomaterials* **2018**, *8*, 322. [[CrossRef](#)]
71. Muhammad, N.; Zia-ur-Rehman; Ali, S.; Meetsma, A.; Shaheen, F. Organotin(IV) 4-methoxyphenylethanoates: Synthesis, spectroscopic characterization, X-ray structures and in vitro anticancer activity against human prostate cell lines (PC-3). *Inorg. Chim. Acta* **2009**, *362*, 2842–2848. [[CrossRef](#)]
72. Holmes, R.R.; Day, R.O.; Chandrasekhar, V.; Vollano, J.F.; Holmes, J.M. Pentacoordinated molecules. 65. Discrete, dimeric, and polymeric structures of triphenyltin esters of chlorobenzoic acids. *Inorg. Chem.* **1986**, *25*, 2490–2494. [[CrossRef](#)]
73. Weng Ng, S.; Kumar Das, V.G.; Syed, A. Organotin esters of 3-benzoylpropionic acid. Crystal structure of triphenyltin(IV) 3-benzoylpropionate, (C₆H₅)₃SnOC(O)(CH₂)₂C(O)C₆H₅. *J. Organomet. Chem.* **1989**, *364*, 353–362. [[CrossRef](#)]
74. Smyth, D.R.; Tiekink, E.R.T. Crystal structure of catena-poly-(μ-dichloroacetato)triphenyltin, [Ph₃Sn(O₂CHCl₂)]_n. *Z. Krist. New Cryst. Struct.* **2000**, *215*, 81–82. [[CrossRef](#)]
75. Ma, C.; Sun, J.; Qiu, L.; Cui, J. The synthesis and characterization of triorganotin carboxylates of 2-mercapto-4-methyl-5-thiazoleacetic acid: X-ray crystal structures of polymeric Me₃Sn[O₂CCH₂(C₄H₃NS)S]SnMe₃ and Ph₃Sn[O₂CCH₂(C₄H₃NS)S]SnPh₃. *J. Inorg. Organomet. Polym. Mater.* **2005**, *15*, 341–347. [[CrossRef](#)]
76. Kaluđerović, G.N.; Paschke, R.; Prashar, S.; Gómez-Ruiz, S. Synthesis, characterization and biological studies of 1-D polymeric triphenyltin(IV) carboxylates. *J. Organomet. Chem.* **2010**, *695*, 1883–1890. [[CrossRef](#)]
77. Śliwka, L.; Wiktorska, K.; Suchocki, P.; Milczarek, M.; Mielczarek, S.; Lubelska, K.; Cierpień, T.; Łyżwa, P.; Kiełbasiński, P.; Jaromin, A.; et al. The comparison of MTT and CVS assays for the assessment of anticancer agent interactions. *PLoS ONE* **2016**, *11*, e0155772. [[CrossRef](#)]
78. Vistica, D.T.; Skehan, P.; Scudiero, D.; Monks, A.; Pittman, A.; Boyd, M.R. Tetrazolium-based assays for cellular viability: A critical examination of selected parameters affecting formazan production. *Cancer Res.* **1991**, *51*, 2515–2520. [[PubMed](#)]
79. Shoemaker, M.; Cohen, I.; Campbell, M. Reduction of MTT by aqueous herbal extracts in the absence of cells. *J. Ethnopharmacol.* **2004**, *93*, 381–384. [[CrossRef](#)]
80. Wang, P.; Henning, S.M.; Heber, D. Limitations of MTT and MTS-based assays for measurement of antiproliferative activity of green tea polyphenols. *PLoS ONE* **2010**, *5*, e10202. [[CrossRef](#)]
81. Bruggisser, R.; von Daeniken, K.; Jundt, G.; Schaffner, W.; Tullberg-Reinert, H. Interference of plant extracts, phytoestrogens and antioxidants with the MTT tetrazolium assay. *Planta Med.* **2002**, *68*, 445–448. [[CrossRef](#)]
82. Vermes, I.; Haanen, C.; Steffens-Nakken, H.; Reutelingsperger, C. A Novel assay for apoptosis. flow cytometric detection of phosphatidylserine expression on early apoptotic cells using fluorescein labelled annexin V. *J. Immunol. Methods* **1995**, *184*, 39–51. [[CrossRef](#)]
83. Edeler, D.; Kaluđerović, M.R.; Dojčinović, B.; Schmidt, H.; Kaluđerović, G.N. SBA-15 mesoporous silica particles loaded with cisplatin induce senescence in B16F10 Cells. *RSC Adv.* **2016**, *6*, 111031–111040. [[CrossRef](#)]
84. Ormerod, M.G.; Orr, R.M.; Peacock, J.H. The role of apoptosis in cell killing by cisplatin: A flow cytometric study. *Br. J. Cancer* **1994**, *69*, 93–100. [[CrossRef](#)] [[PubMed](#)]
85. Ormerod, M.G.; O'Neill, C.; Robertson, D.; Kelland, L.R.; Harrap, K.R. Cis-diamminedichloroplatinum(II)-induced cell death through apoptosis in sensitive and resistant human ovarian carcinoma cell lines. *Cancer Chemother. Pharmacol.* **1996**, *37*, 463–471. [[CrossRef](#)] [[PubMed](#)]
86. Siddik, Z.H. Cisplatin: Mode of cytotoxic action and molecular basis of resistance. *Oncogene* **2003**, *22*, 7265–7279. [[CrossRef](#)] [[PubMed](#)]
87. Predarska, I.; Saoud, M.; Drača, D.; Morgan, I.; Komazec, T.; Eichhorn, T.; Mihajlović, E.; Dunderović, D.; Mijatović, S.; Maksimović-Ivanić, D.; et al. Mesoporous silica nanoparticles enhance the anticancer efficacy of platinum(IV)-phenolate conjugates in breast cancer cell lines. *Nanomaterials* **2022**, *12*, 3767. [[CrossRef](#)] [[PubMed](#)]
88. Choi, Y.-M.; Kim, H.-K.; Shim, W.; Anwar, M.A.; Kwon, J.-W.; Kwon, H.-K.; Kim, H.J.; Jeong, H.; Kim, H.M.; Hwang, D.; et al. Mechanism of cisplatin-induced cytotoxicity is correlated to impaired metabolism due to mitochondrial ROS generation. *PLoS ONE* **2015**, *10*, e0135083. [[CrossRef](#)] [[PubMed](#)]
89. Kleih, M.; Böppele, K.; Dong, M.; Gaißler, A.; Heine, S.; Olayioye, M.A.; Aulitzky, W.E.; Essmann, F. Direct impact of cisplatin on mitochondria induces ROS production that dictates cell fate of ovarian cancer cells. *Cell Death Dis.* **2019**, *10*, 851. [[CrossRef](#)]
90. Zuo, J.; Zhang, Z.; Li, M.; Yang, Y.; Zheng, B.; Wang, P.; Huang, C.; Zhou, S. The crosstalk between reactive oxygen species and noncoding RNAs: From cancer code to drug role. *Mol. Cancer* **2022**, *21*, 30. [[CrossRef](#)]
91. Moncada, S.; Palmer, R.M.; Higgs, E.A. Nitric oxide: Physiology, pathophysiology, and pharmacology. *Pharmacol. Rev.* **1991**, *43*, 109–142.

92. Thomas, D.D.; Ridnour, L.A.; Isenberg, J.S.; Flores-Santana, W.; Switzer, C.H.; Donzelli, S.; Hussain, P.; Vecoli, C.; Paolocci, N.; Ambs, S.; et al. The chemical biology of nitric oxide: Implications in cellular signaling. *Free Radic. Biol. Med.* **2008**, *45*, 18–31. [[CrossRef](#)]
93. Hickok, J.R.; Thomas, D.D. Nitric oxide and cancer therapy: The emperor has no clothes. *Curr. Pharm. Des.* **2010**, *16*, 381–391. [[CrossRef](#)] [[PubMed](#)]
94. Khan, F.H.; Dervan, E.; Bhattacharyya, D.D.; McAuliffe, J.D.; Miranda, K.M.; Glynn, S.A. The role of nitric oxide in cancer: Master regulator or not? *Int. J. Mol. Sci.* **2020**, *21*, 9393. [[CrossRef](#)] [[PubMed](#)]
95. Xu, W.; Liu, L.Z.; Loizidou, M.; Ahmed, M.; Charles, I.G. The role of nitric oxide in cancer. *Cell Res.* **2002**, *12*, 311–320. [[CrossRef](#)] [[PubMed](#)]
96. Eyler, C.E.; Wu, Q.; Yan, K.; MacSwords, J.M.; Chandler-Militello, D.; Misuraca, K.L.; Lathia, J.D.; Forrester, M.T.; Lee, J.; Stamler, J.S.; et al. Glioma stem cell proliferation and tumor growth are promoted by nitric oxide synthase-2. *Cell* **2011**, *146*, 53–66. [[CrossRef](#)] [[PubMed](#)]
97. Massi, D.; Franchi, A.; Sardi, I.; Magnelli, L.; Paglierani, M.; Borgognoni, L.; Maria Reali, U.; Santucci, M. Inducible nitric oxide synthase expression in benign and malignant cutaneous melanocytic lesions. *J. Pathol.* **2001**, *194*, 194–200. [[CrossRef](#)]
98. Ambs, S.; Merriam, W.G.; Bennett, W.P.; Felley-Bosco, E.; Ogunfusika, M.O.; Oser, S.M.; Klein, S.; Shields, P.G.; Billiar, T.R.; Harris, C.C. Frequent nitric oxide synthase-2 expression in human colon adenomas: Implication for tumor angiogenesis and colon cancer progression. *Cancer Res.* **1998**, *58*, 334–341.
99. Okayama, H.; Saito, M.; Oue, N.; Weiss, J.M.; Stauffer, J.; Takenoshita, S.; Wiltrout, R.H.; Hussain, S.P.; Harris, C.C. NOS2 Enhances KRAS-induced lung carcinogenesis, inflammation and MicroRNA-21 expression. *Int. J. Cancer* **2013**, *132*, 9–18. [[CrossRef](#)]
100. Thomsen, L.L.; Miles, D.W.; Happerfield, L.; Bobrow, L.G.; Knowles, R.G.; Moncada, S. Nitric oxide synthase activity in human breast cancer. *Br. J. Cancer* **1995**, *72*, 41–44. [[CrossRef](#)]
101. Glynn, S.A.; Boersma, B.J.; Dorsey, T.H.; Yi, M.; Yfantis, H.G.; Ridnour, L.A.; Martin, D.N.; Switzer, C.H.; Hudson, R.S.; Wink, D.A.; et al. Increased NOS2 predicts poor survival in estrogen receptor-negative breast cancer patients. *J. Clin. Investig.* **2010**, *120*, 3843–3854. [[CrossRef](#)]
102. Bulut, A.S.; Erden, E.; Sak, S.D.; Doruk, H.; Kursun, N.; Dincol, D. Significance of inducible nitric oxide synthase expression in benign and malignant breast epithelium: An immunohistochemical study of 151 cases. *Virchows Arch.* **2005**, *447*, 24–30. [[CrossRef](#)]
103. Loibl, S.; Buck, A.; Strank, C.; von Minckwitz, G.; Roller, M.; Sinn, H.-P.; Schini-Kerth, V.; Solbach, C.; Strebhardt, K.; Kaufmann, M. The role of early expression of inducible nitric oxide synthase in human breast cancer. *Eur. J. Cancer* **2005**, *41*, 265–271. [[CrossRef](#)]
104. Granados-Principal, S.; Liu, Y.; Guevara, M.L.; Blanco, E.; Choi, D.S.; Qian, W.; Patel, T.; Rodriguez, A.A.; Cusimano, J.; Weiss, H.L.; et al. Inhibition of iNOS as a novel effective targeted therapy against triple-negative breast cancer. *Breast Cancer Res.* **2015**, *17*, 25. [[CrossRef](#)] [[PubMed](#)]
105. Hinz, B.; Brune, K.; Rau, T.; Pahl, A. Flurbiprofen enantiomers inhibit inducible nitric oxide synthase expression in RAW 264.7 macrophages. *Pharm. Res.* **2001**, *18*, 151–156. [[CrossRef](#)] [[PubMed](#)]
106. Afshari Behbahanizadeh, S.; Farashi Bonab, S. Study the effect of indomethacin administration on breast tumor growth and INOS gene expression in tumor-bearing mice. *Int. J. Adv. Biol. Biomed. Res.* **2019**, *7*, 160–172. [[CrossRef](#)]
107. Chen, Y.; McMillan-Ward, E.; Kong, J.; Israels, S.J.; Gibson, S.B. Oxidative stress induces autophagic cell death independent of apoptosis in transformed and cancer cells. *Cell Death Differ.* **2008**, *15*, 171–182. [[CrossRef](#)]
108. Muniraj, N.; Siddharth, S.; Shriver, M.; Nagalingam, A.; Parida, S.; Woo, J.; Elsey, J.; Gabrielson, K.; Gabrielson, E.; Arbiser, J.L.; et al. Induction of STK11-dependent cytoprotective autophagy in breast cancer cells upon honokiol treatment. *Cell Death Discov.* **2020**, *6*, 81. [[CrossRef](#)] [[PubMed](#)]

Disclaimer/Publisher’s Note: The statements, opinions and data contained in all publications are solely those of the individual author(s) and contributor(s) and not of MDPI and/or the editor(s). MDPI and/or the editor(s) disclaim responsibility for any injury to people or property resulting from any ideas, methods, instructions or products referred to in the content.